A study on inelastic constitutive law for design purpose considering non-linear plasticity

T.Igari
Nagasaki R & D Center, Mitsubishi Heavy Industries Ltd, Japan
H.Koto
Takasago R & D Center, Mitsubishi Heavy Industries Ltd, Japan
H.Wada
Kobe Shipyard & Engine Works, Mitsubishi Heavy Industries Ltd, Japan
Y.Asada
University of Tokyo, Japan

1. INTRODUCTION

In the inelastic analysis for the rational designing of high temperature structures, the constitutive equation plays a very important role. For the fast breeder reactor design analyses, ORNL's tenth-cycle-hardening model with bilinear stress-strain representation has been used widely because of its simplicity and compatibility with general purpose FEM codes.

However, the following shortcomings of the model have been pointed out. i) It is difficult to determine the proper value of plastic work-hardening constant because strain distribution exists in the structure. ii) Since the cyclic hardening/softening characteristics of the material are oversimplified, the calculated stress and strain under cyclic loading conditions tend to be inaccurate and may lead to unreliable life prediction.

On the other hand, new constitutive equations such as nonlinear plasticity models (Ohno & Kachi 1985) and unified models (Chaboche & Rousselier 1983) have been proposed and efforts to apply these models to practical problems are continued. But there are few applications of these models to actual design analyses at present, because some difficulties remain for determining material constants and coding them into FEM codes.

The constitutive model, which is easily applicable to structure analysis and at the same time accurate enough for design purpose, was proposed by the authors (Koto et al. 1987). First, in the present paper, the model is reviewed briefly. Secondly, some kinds of inelastic behaviors are analized by the model and the results are compared with experiments in order to examine an applicability of the model.

2. FEATURES OF THE PRESENT CONSTITUTIVE MODEL

The conventional approach of separating plastic and creep strains is followed in this paper. As for creep itself, the ORNL's modified hardening rule is adopted. We make some refinements in the description of the plastic behavior including its interaction with creep. The basic equations on the plasticity used in the present model are summarized in Table 1. The features of the present model are as follows.

2.1 Nonlinear plasticity model

Masing model (Igari et al. 1983) is adopted to represent the nonlinear plastic behavior. This model is based on the stress-plastic strain relationship, whose origin is updated at every plastic reversal, as shown in Fig.1. In Fig.1, neglecting the cyclic hardening/softening behavior, the relations between the functions f_M and f_H, as well as the functions H_M and H_H are expressed as follows;

(1) $$f_H(\tilde{\varepsilon}_p) = 2 \cdot f_M(\tilde{\varepsilon}_p/2)$$

(2) $$H_H(\tilde{\varepsilon}_p) = H_M(\tilde{\varepsilon}_p/2)$$

The plastic reversal is assumed to occur when the following inequality is satisfied.

(3) $$(S_{ULij} - \alpha_{ij}) \cdot dS_{ij} < 0$$

where S_{ULij} and α_{ij} indicate the deviatoric stress just before elastic unloading and the center of the yield surface, respectively, and dS_{ij} is the increment of deviatoric stress at re-yielding. Using this reversal point "Porigin", $\tilde{\varepsilon}_p$ is represented by

(4) $$\tilde{\varepsilon}_p = \int_{P_{origin}} \left(\frac{2}{3} d\varepsilon^P_{ij}\, d\varepsilon^P_{ij}\right)^{\frac{1}{2}}$$

Moreover, the concept of the hardened strain region is introduced in order to improve the Masing model for the case of over-straining after constant strain range cycling as shown in Fig.2.
The hardened strain region is defined by the function g as follows;

(5) $$g = \frac{2}{3} \varepsilon^P_{ij} \varepsilon^P_{ij} - \rho^2$$

(6) $$d\rho = \sqrt{\frac{2}{3}} \frac{(\partial g / \partial \varepsilon^P_{ij})\, d\varepsilon^P_{ij}}{\{(\partial g / \partial \varepsilon^P_{K\ell})(\partial g / \partial \varepsilon^P_{K\ell})\}^{\frac{1}{2}}} \cdot I$$

(7) $$I = \begin{cases} 1, & g = 0 \text{ and } \varepsilon^P_{ij} \cdot d\varepsilon^P_{ij} \geq 0 \\ 0, & g < 0 \text{ or } \varepsilon^P_{ij} \cdot d\varepsilon^P_{ij} < 0 \end{cases}$$

The slope of stress-plastic strain curve is expressed by the state of the function g.

(8) $$H = \begin{cases} H_M(\tilde{\varepsilon}_p) & , \quad g = 0 \\ H_H(\tilde{\varepsilon}_p) = H_M(\tilde{\varepsilon}_p/2), & \quad g < 0 \end{cases}$$

2.2 Continuous cyclic hardening/softening representation

The cyclic hardening/softening characteristics is represented by the cyclic hardening/softening factor R, which means the ratio of the monotonic and cyclic stresses. Using the factor R, hysteresis curve in the constant strain range cycling test is indicated as follows:

(9) $$\tilde{\sigma} = R \cdot f_H(\tilde{\varepsilon}_p) = 2 \cdot R \cdot f_M(\tilde{\varepsilon}_p/2)$$

where, $$R \begin{cases} =1, & \text{without cyclic hardening/softening} \\ >1, & \text{for cyclic hardening} \\ <1, & \text{for cyclic softening} \end{cases}$$

Cyclic hardening/softening is often characterized by the accumulated plastic strain $\overline{\varepsilon_p}$ (= $\int(\frac{2}{3}d\varepsilon^P_{ij}\, d\varepsilon^P_{ij})^{\frac{1}{2}}$):

$$R = R(\overline{\varepsilon_p}) \tag{10}$$

Fig.3 shows the examples of such experimental data. The data of normarized and tempered 2 1/4Cr-1Mo steel fall within a relatively narrow band. However, for 304 stainless steel, the dependency of strain range is observed. In order to simplify the treatment of such strain-range dependency, we introduce accumulated effective plastic strain to cyclic hardening, $\overline{\varepsilon_{p,eff}}$, which is defined by the following equations (See Fig.4).

$$\widetilde{\varepsilon_{p,eff}} = \begin{cases} 0 & , \quad \tilde{\varepsilon}_p \le \tilde{\varepsilon}_s \\ \tilde{\varepsilon}_p - \tilde{\varepsilon}_s & , \quad \tilde{\varepsilon}_p > \tilde{\varepsilon}_s \end{cases} \tag{11}$$

$$\overline{\varepsilon_{p,eff}} = \Sigma\ \widetilde{\varepsilon_{p,eff}} \tag{12}$$

In eq. (11), $\tilde{\varepsilon}_s$ is the plastic strain which has no effect for cyclic hardening, and can be estimated from the following equation.

$$R_r = f_c(\tilde{\varepsilon}_s/2)/f_M(\tilde{\varepsilon}_s/2) \tag{13}$$

where, Rr is the current hardening level at the plastic reversal and f_c is the function of the cyclic stress-strain relation ($\Delta\tilde{\sigma}/2=f_c(\Delta\tilde{\varepsilon}_p/2)$, $\Delta\tilde{\sigma}$: saturated stress range). The data of 304 stainless steel in Fig.3 are re-plotted by the relationship between factor R and $\overline{\varepsilon_{p,eff}}$ as shown in Fig.5. The strain range dependency is found to be small in this figure, therefore eq.(10) can be written as follow independent of the strain range.

$$R = R(\overline{\varepsilon_{p,eff}}) \tag{14}$$

According to the above procedure, $\tilde{\varepsilon}_s$ in the cycling test of constant plastic strain range continues to increase with plastic reversal until it reaches the plastic strain range, because Rr in eq.(13) increases along the R-$\overline{\varepsilon_{p,eff}}$ curve in Fig.4 (b). Therefore, $\widetilde{\varepsilon_{p,eff}}$ decreases to zero, as $\tilde{\varepsilon}_s$ increases to the plastic strain range. Thereafter, factor R stays at a saturation value Rs depending on the plastic strain range.

2.3 Plasticity-creep interaction

Plasticity-creep interaction is taken into account to some extent based on both experimental observations and consideration of the correspondence to the unified theories. That is to say, plastic strain ε_p is replaced by inelastic strain ε_{in} ($=\varepsilon_p + \varepsilon_c$) in the plasticity constitutive equation. Consequently, translation of the yield surface by creep strains, change of the slope of stress-strain curve by creep strains and acceleration of cyclic hardening/softening by creep strains are considered. The effect of prior plasticity on subsequent creep is also considered by the β-option method (Pugh et al. 1977). The effect of loading rate on stress-strain behavior is represented as the creep strain effect.

3. COMPARISON WITH EXPERIMENTAL RESULTS

The following material behaviors are analized and the results are compared with experiments in order to examine an applicability of the model.

i) Combined tension-torsion test under non-proportional loading condition.
The calculations by the proposed model and bi-linear model are compared with experiments (Shiratori et al. 1981) in Fig.6. The calculations by the proposed model show the transient nonlinear stress-strain behaviors in non-proportional loading similar to experiments. The applicability of the definition of plastic reversal in eq.(3) to non-proportional loading is clarified.
ii) Varying strain-range cycling test under uniaxial condition.
Fig.7 shows the change of stress-range in this test. Good agreement is seen between experiment and prediction. This model can express the cylic hardening characteristics including the strain-range dependency. That is, as mentioned before, factor R increases along $R-\overline{\varepsilon_{p,eff}}$ curve until $\tilde{\varepsilon}_s$ reaches plastic strain range. As the result, not only the saturated stress but the hardening rate is well simulated in Fig.7.
iii) Strain cycling test with varying mean-strain under uniaxial condition.
Fig.8 shows comparison between experimental and predicted stress-strain hysteresis loop. It is seen that the proposed model can predict the experimental behavior rather successfully than bi-linear model, because of the nonlinear stress-strain representation and the introduction of the hardened strain region concept.

4. SUMMARY

The validity of the proposed model in describing the nonlinear stress-strain relationship and cyclic hardening/softening behavior was examined by comparison with experimental behaviors. The analytical results coincided well with experimental ones, and the applicability of the model to cyclic inelastic deformation appearing in the design of FBR components was clarified. This model is applied to the inelastic design analyses of FBR components with the procedures of creep-fatigue life evaluation (Sakon et al. 1987), and the examples of the results are presented in this conference (Wada et al. 1987 and Sohman et al. 1987).

REFERENCES

Ohno, N. & Kachi, Y. 1985. Proc. 8th SMiRT Conf. : L2/2
Chaboche, J.L. & Rousselier, G. 1983. Trans. ASME-J. Press. Vessel. Techn. 105:153-164.
Koto, H., Igari, T., Nakamura, K., Wada, H. & Asada, Y. 1987. Proc. 2nd Int. Conf. on Constitutive Laws in Arizona, p.597-604 : Elsevier
Igari, T., Setoguchi, K. & Yamauchi, M. 1983. J. Soc. Mat. Sci. 32 : 610-614 (in Japanese)
Shiratori, E. et al. 1981. Trans. JSME-Series A 47:441-449 (in Japanese)
Corum, J.M. & Pugh, C.E. 1977. ORNL-5281
Sakon, T., Wada, H. & Asada, Y. 1987. Proc. 9th SMiRT Conf. : L6/7
Wada, H., Sohman, Y. & Nakamura, K. 1987. Proc. 9th SMiRT Conf. : E8/1
Sohman, Y., Wada, H. & Igari, T. 1987. Proc. 9th SMiRT Conf. : E7/2

Table 1 Summary of basic equations on plasticity

Plasticity

• Yield function

$$F=\frac{3}{2}(S_{ij}-\alpha_{ij})(S_{ij}-\alpha_{ij})-(R\cdot\sigma_p)^2=0$$

$$R=R(\overline{\varepsilon_{in,eff}}),\quad \sigma_p=\sigma_p(T)$$

σ_p ···size of the yield surface for virgin material

T···temperature

• Flow rule

$$d\varepsilon_{ij}^{p}=\Lambda\frac{\partial F}{\partial S_{ij}}$$

$$\Lambda=\frac{\frac{\partial F}{\partial S_{k\ell}}dS_{k\ell}-2R\sigma_p\left(\sigma_p\frac{\partial R}{\partial \overline{\varepsilon_{in,eff}}}d\overline{\varepsilon_{in,eff}}+R\frac{\partial \sigma_p}{\partial T}dT\right)}{\frac{2}{3}H\frac{\partial F}{\partial S_{mn}}\frac{\partial F}{\partial S_{mn}}}$$

$$H=H(\widetilde{\varepsilon_{in}})$$

• Hardening rule

$$d\alpha_{ij}=\frac{2}{3}Hd\varepsilon_{ij}^{in}$$

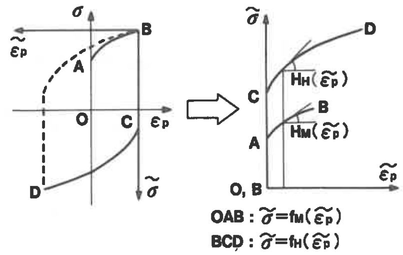

Fig.1 Schema of Masing model

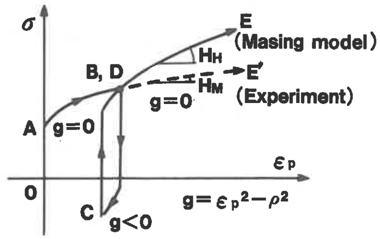

Fig.2 Loading to a large strain after cycling

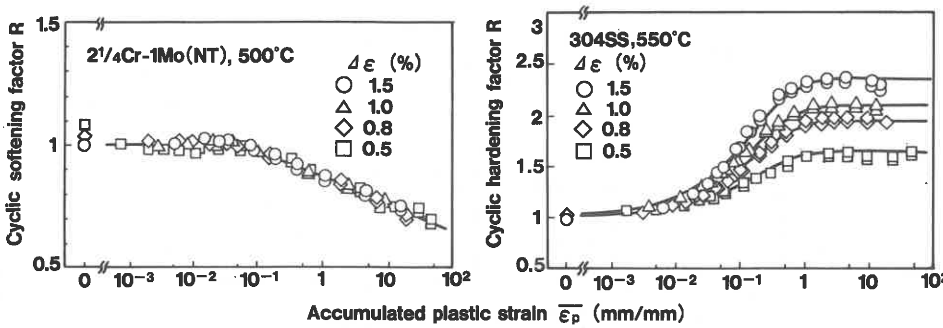

Fig.3 Relationship between factor R and accumulated plastic strain $\overline{\varepsilon_p}$

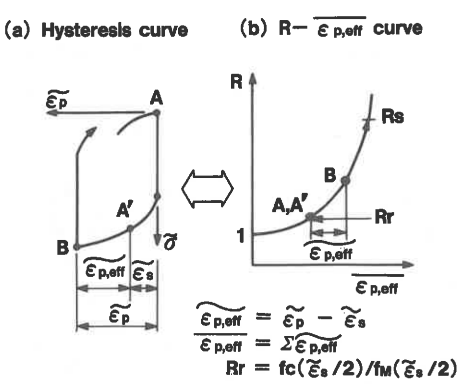

Fig.4 Accumulated plastic strain effective to cyclic hardening, $\overline{\varepsilon_{p,eff}}$

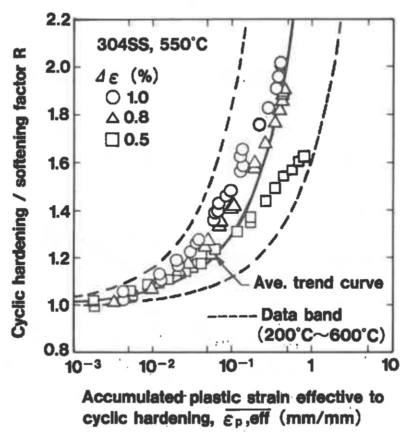

Fig.5 Relationship between factor R and $\overline{\varepsilon_{p,eff}}$

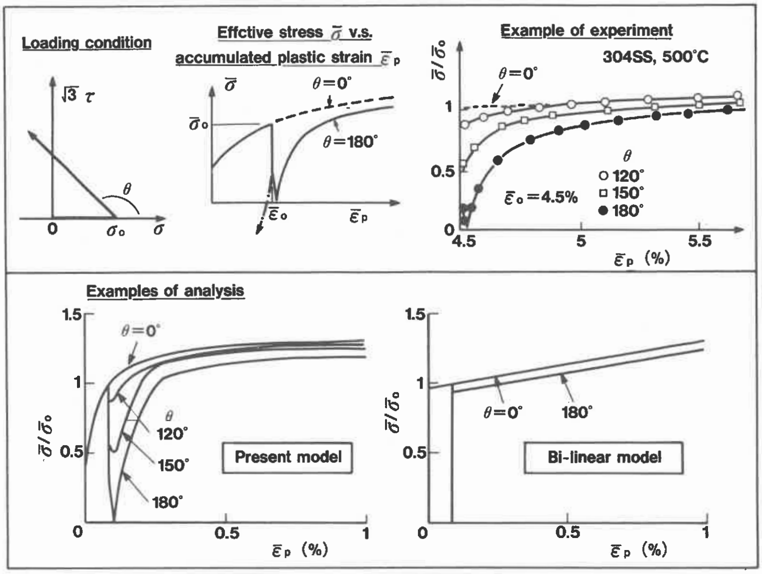

Fig.6 Example of an application to non-proportional loading

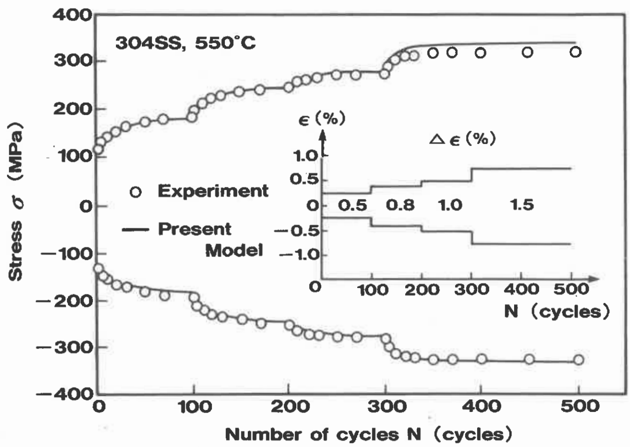

Fig.7 Changes of peak stress under varying strain-range cycling

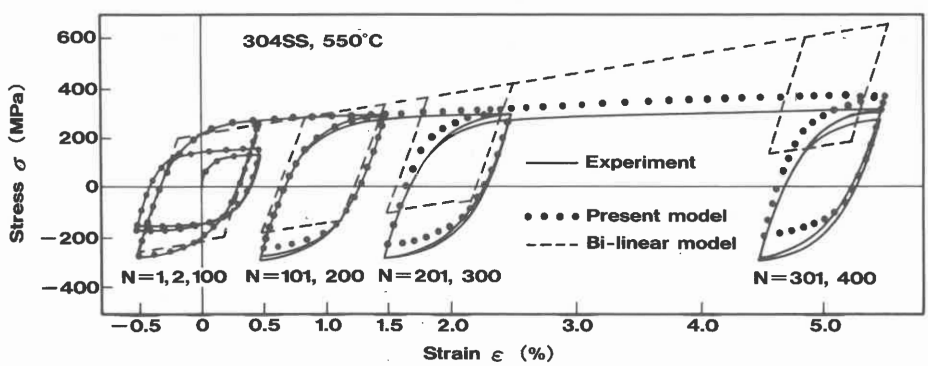

Fig.8 Hysteresis loop of strain cycling with varying mean-strain